Control of PKM machine tools using piezoelectric self-sensing actuators on basis of the functional principle of a scale with a vibrating string

Christian Rudolf[1]*, Thomas Martin[2] and Jörg Wauer[1]

[1]*Institut für Technische Mechanik (ITM), Universität Karlsruhe (TH), Kaiserstr. 10, 76131 Karlsruhe, Germany*
[2]*Forschungszentrum Karlsruhe GmbH, Institut für Angewandte Informatik (IAI)*
Hermann-von-Helmholtz-Platz 1, 76344 Eggenstein-Leopoldshafen, Germany

Abstract. An adaptronic strut for machine tools with parallel kinematics for compensation of the influence of geometric errors is introduced. Implemented within the strut is a piezoelectric sensor-actuator unit separated in function. In the first part of this contribution, the functional principle of the strut is presented. For use of one piezoelectric transducer as both, sensor and actuator as so-called self-sensing actuator, the acquisition of the sensing signal while actuating simultaneously using electrical bridge circuits as well as filter properties are examined. In the second part the control concept developed for the adaptronic strut is presented. A co-simulation model of the strut for simulating the controlled multi-body behavior of the strut is set-up. The control design for the strut as a stand-alone system is tested under various external loads. Finally, the strut is implemented into a model of the complete machine tool and the influence of the controlled strut onto the behavior of the machine tool is examined.

Keywords: parallel kinematics; self-sensing piezo actuator; control; vibrating string.

1. Introduction

In machine tools with parallel kinematics of two or three translational degrees of freedom, as shown exemplarily in Fig. 1, geometric errors in parts of the machine tool, such as assembly errors or differing geometries due to production tolerances, lead to stresses within the structure. These stresses result in deflections of the tool center point (TCP) reducing the quality of the workpiece. For compensation of these deflections an adaptronic strut as depicted in Fig. 2 has been developed. The strut is similar in shape to a conventional strut of machine tools with parallel kinematics. Cut in two halves with a piezoceramic transducer in-between the strut is variable in length. Thus, an additional degree of freedom for compensation has been achieved.

The piezoelectric transducer shall be used as self-sensing actuator fulfilling both functions, sensing and actuating. In the first design step of the strut these two functions are still separated by using two piezoelectric elements. However, using electric circuits, e.g. bridge circuits, the sensing signal can be acquired while actuating at the same time.

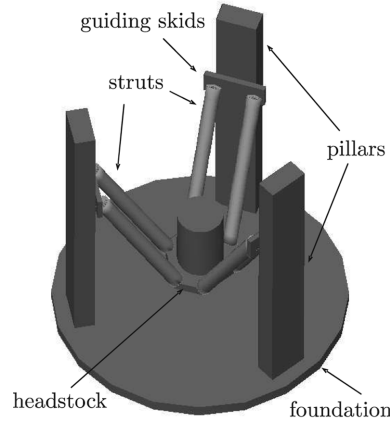*Corresponding Author, E-mail: rudolf@itm.uni-karlsruhe.de

Fig. 1 Parallel kinematic machine tool with three translational degrees of freedom, Rudolf, *et al*. (2007)
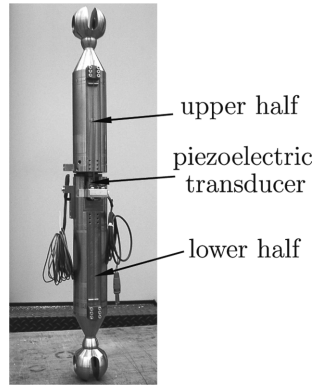

Fig. 2 Adaptronic strut, Rudolf, *et al*. (2005)

The considered deflections are static and sometimes quasi-static, and thus, they induce only static or quasi-static signals within the piezoelectric transducer. However, due to the discharging resistance of the piezoelectric material these signals are not measurable according to Bill (2002), Ruschmeyer (1995).

Therefore, a work-around based on the functional principle of a scale with a vibrating string was designed Rudolf, *et al*. (2005). A string mounted along the strut is excited by a solenoid inducing a dynamic signal onto the piezoelectric element. This signal can be aquired and its frequency can be determined using frequency counters or phase-locked loops (PLL). Using the Eq. (1) between the eigenfrequency f_0 of the string and the prestress T on the string

$$f_0 = \frac{1}{2l_S}\sqrt{\frac{T}{A\rho}}, \tag{1}$$

with l_S, A and ρ being length, cross-sectional area and density of the string, respectively, the external static or quasi-static load on the strut can be determined. Further information about the functional principle of the adaptronic strut can be found in Fleischer, *et al*. (2006) and Rudolf, *et al*. (2005, 2006).

Within this contribution we only marginally consider the electromechanical relations of the piezoelectric transducer between force, electric field as well as mechanical and electrical displacement. For the stack actuator used, applying Einstein's summation rule, the linear constitutive equations

$$T_p = c_{pq}^E S_q - e_{kp} E_k \tag{2}$$

$$D_p = e_{pq} S_q + \varepsilon_{kp}^S E_k \tag{3}$$

with $p \in \{1,2,3\}$ hold for small voltage signals, where T_p and S_q are stress and strain and E_k and D_p are electric field and electric displacement in the piezoelectric material. These system variables are related with each other by the piezoelectric constants e_{kp}, permittivity ε_{kp}^S at constant mechanical stress S and elasticity constant c_E^{pq} at constant electrical field E. In case large signal behavior must be considered during realization of the adaptronic strut the hysteretic dependency between, for example, voltage and force can be described using elementary operators such as lefthanded and righthanded saturation, hysteresis (or backlash) and creep operators. Their non-linear behavior can be made linear by compensation using inverse control, see Janocha and Kuhnen (2000, 2006) and Kuhnen and Janocha (2001).

The first part of this contribution deals with piezoelectric self-sensing effects and the examination and assessment of the different possible electric circuits for separating actuation and sensing signal of the piezoelectric transducer to achieve these effects. Within the second part, starting with a lumped mass model of the strut, the design of an appropriate control concept for the adaptronic strut is presented. Firstly, the concept is evaluated on a model for the strut as a stand-alone system under external loads, and secondly, the strut model is implemented into the model of the machine tool and its influence on the behavior of the machine tool is treated.

2. Piezoelectric self-sensing

A signal representing the string vibration can be obtained with the piezoelectric transducer when operated as a self-sensing actuator. The desired frequency information is contained in the superposed dynamic load of the vibrating string on the transducer. For the considered application it is in a range of 4 to 6 kHz whereas static forces and corresponding driving signals to the actuator are in a frequency range up to 1 kHz. The difference of their frequency ranges is an essential condition for the separation of process loads and loads on the transducer due to the vibrating string.

2.1. Methods for self-sensing the string vibration

One approach to obtain the high-frequency signal of the vibrating string is, first, to gain the overall load on the transducer by operating it in a self-sensing configuration and, second, filter this signal for the known frequency range of the string vibration.

Common methods of using piezoelectric transducers as self-sensing actuators employ bridge circuits, such as the capacitive bridge circuit exemplarily shown in Fig. 3, to determine the force-induced charge component q_F or strain-induced charge component q_S. The bridge voltage

$$V_{out}(jw) = \left(\frac{Z_{r2}}{Z_{p2} + Z_{r2}} - \frac{Z_{r1}}{Z_{p1} + Z_{r1}} \right) V_{in}(jw) + \frac{Z_{p1} Z_{r1}}{Z_{p1} + Z_{r1}} jw q_F(jw) \tag{4}$$

described in the frequency domain with complex electric impedances

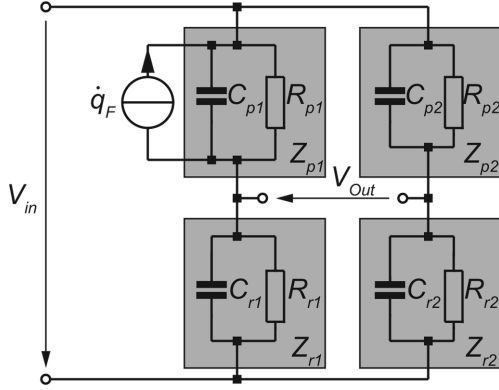$$Z = \frac{1}{jwC + \frac{1}{R}} \tag{5}$$

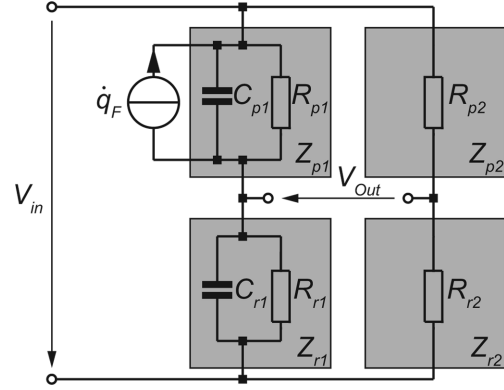Fig. 3 Capacitive bridge circuit for piezoelectric self-sensing

Fig. 4 Bridge circuit with purely resistive reference branch for piezoelectric self-sensing

gets independent of the driving voltage V_{in} if the equilibrium conditions

$$Z_{p1} = Z_{p2} \quad \text{and} \quad Z_{r1} = Z_{r2} \tag{6}$$

are fulfilled, reducing (4) to

$$V_{out} = \frac{Z_{p1}Z_{r1}}{Z_{p1} + Z_{r1}} jw q_F(jw). \tag{7}$$

These conditions (6) are fulfilled by choosing

$$C_{p2} = C_{p1}, C_{r2} = C_{r1}, R_{p2} = R_{p1} \text{ and } R_{r2} = R_{r1}. \tag{8}$$

However, this adjustment has shown to be quite cumbersome in practice as slight deviations dramatically impair results, Babuška and O'Donnell (1998). A version of the bridge circuit which is easier to handle is shown in Fig. 4. For conditions

$$\frac{R_{p1}}{R_{r1}} = \frac{C_{r1}}{C_{p1}} \tag{9}$$

and

$$\frac{R_{p2}}{R_{r2}} = \frac{C_{r1}}{C_{p1}} \tag{10}$$

Eq. (4) reduces to Eq. (7) as well, becoming independent of the driving voltage V_{in}.

In this configuration only resistances have to be adjusted which is more easily accomplished in practice than matching capacitances as it is required in Eq. (8). As a downside, however, the threshold frequency at which dynamic loads can be measured will be raised if R_{p1} is lowered to meet Eq. (9). For the considered application, however, this is not an issue since high-frequency signal parts are of interest and high-pass filtering has to be applied in the signal processing chain anyway.

Both bridge circuits described above are based on a linear model of the piezoelectric transducer since constant capacitances and resistances are used for balancing. To overcome this downside the usage of an identical unloaded piezoelectric transducer instead of the constant capacitance C_{p2} in the reference branch of the bridge in Fig. 3 has been suggested by Jones, *et al.* (1994).
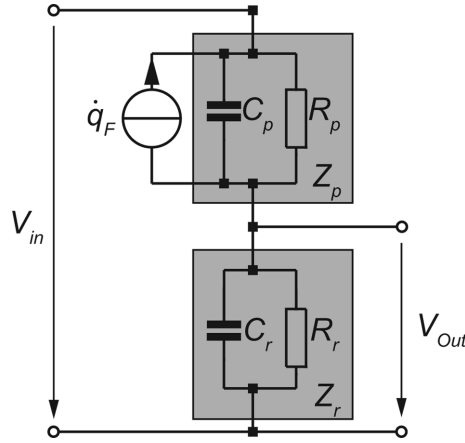
Fig. 5 Sawyer-Tower circuit for charge measurement

Another approach to obtain the vibration frequency of the string is to measure the charge on the transducer and pass this signal through a frequency filter to extract the high-frequency component induced by the corresponding high-frequency loads. To measure the charge on the transducer a Sawyer-Tower circuit as depicted in Fig. 5 can be employed.

Since the amplitude of the wanted frequency range will be very low in this signal and the difference between wanted and dominant frequencies is only about half of a decade a frequency filter with high rolloff and therefore high order has to be used. However, on one hand high filter orders induce a phase shift that might be unfavorable in dynamic control applications. On the other hand no adjustments as with bridge circuits are required for this configuration.

Frequency filtering of the signal obtained by either bridge circuits or charge measurement can be accomplished by a high-pass filter. Unwanted frequencies above 6 kHz, however, e.g. originating from resonant vibration of the piezoelectric transducer, which might disturb the detection of the frequency of the vibrating string will be passed through the filter as well. Therefore, an appropriate band-pass filter might be necessary instead.

2.2. Experimental set-up

To verify the proposed concepts of a self-sensing actuator for extracting the vibration frequency of the string experiments were conducted on a test rig. It consists of two piezoelectric multilayer bending actuators (both of type PL140.00 by PI (Physik Instrumente) GmbH & Co. KG). One of them is operated as self-sensing actuator placed into the different configurations described above, the other one is mechanically coupled to the first one imposing an external force of sinusoidal form onto its tip.

This load is corresponding to the force induced by the string vibration on the strut. Since the force between the actuators results from the interaction of both bending transducers the overall load on the self-sensing actuator contains a second component due to the actuation of the self-sensing actuator. This load component corresponds to the process load in the strut.

Since the piezoelectric bending actuators in the experimental set-up are characterized by low resonant frequencies of around 160 Hz the frequencies of the envisaged application could not be applied in the test rig. Instead a proportional frequency range of up to 10 Hz for the driving voltage V_{in} of the self-sensing actuator and between 40 and 60 Hz for the external vibrational force was used. For V_{in} the
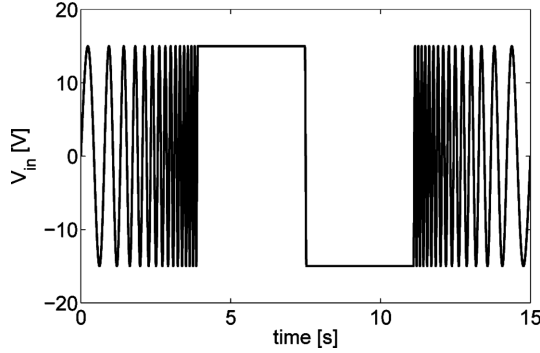
Fig. 6 Test signal for the driving voltage V_{in} of the piezoelectric self-sensing actuator
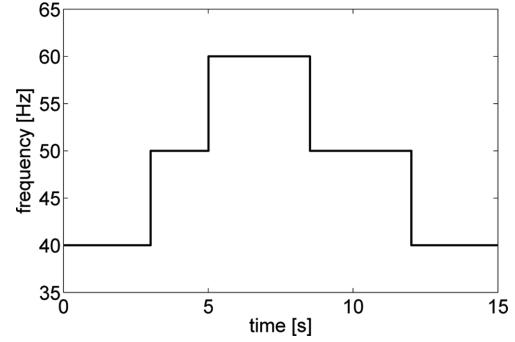

Fig. 7 Frequency course of the external vibrational force generated by the second piezoelectric transducer

symmetric test signal depicted in Fig. 6 was used. It contains two sinusoidal logarithmic chirp waveforms from 1 μHz to 10 Hz and vice versa as well as two DC-sections joined at $t = 7.5$ s by half of a period of a cosine at 10 Hz. The second actuator generating the external vibrational force was driven by a sinusoidal voltage signal whose frequency follows the course shown in Fig. 7.

2.3. Experimental results

Three different self-sensing bridge circuits were investigated: The capacitive bridge circuit shown in Fig. 3, a capacitive bridge circuit with a third identical unloaded piezoelectric bending transducer instead of the constant reference capacitance C_{p2}, and the bridge circuit with a purely resistive reference branch depicted in Fig. 4. The bridge voltage V_{out} was passed through a fourth-order Butterworth-band-pass filter with cut-off frequencies of 35 and 65 Hz.

In addition to the bridge circuits a Sawyer-Tower circuit for charge measurement was investigated. The measured voltage V_{out} had to be passed through an eighth-order Butterworth-band-pass filter with cut-off frequencies of 35 and 65 Hz to obtain signals that were comparable to those of the bridge circuits.

To visualize the frequency information contained in the resulting signals of all tests a frequency-time-plot was created by determining the frequency as the inverse of twice the time between zero crossings.
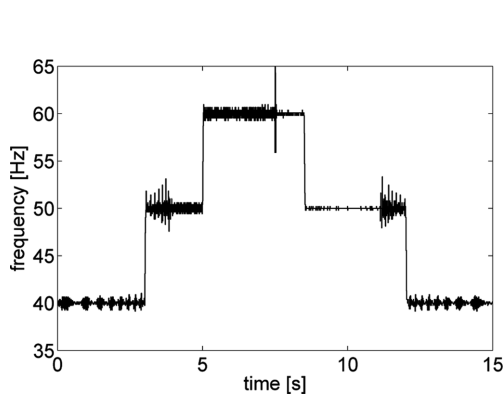

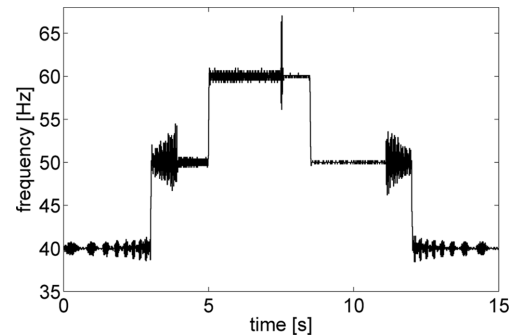Fig. 8 Frequency extracted with capacitive bridge circuit

Fig. 9 Frequency extracted with capacitive bridge circuit with piezoelectric transducer instead of constant reference capacitance C_{p2}
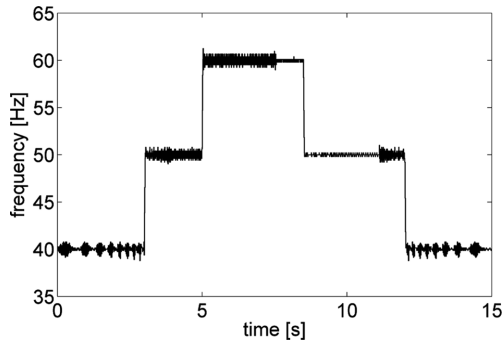
Fig. 10 Frequency extracted with bridge circuit with resistive reference branch
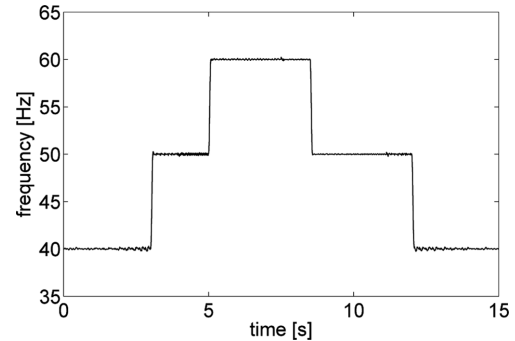
Fig. 11 Averaged frequency extracted with bridge circuit with resistive reference branch
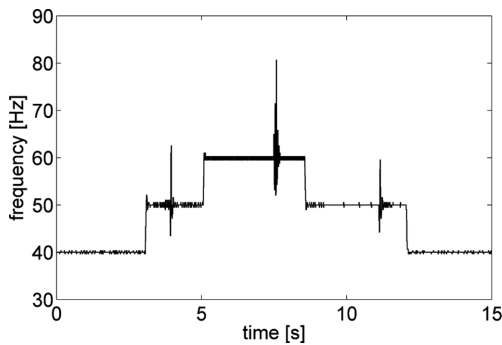
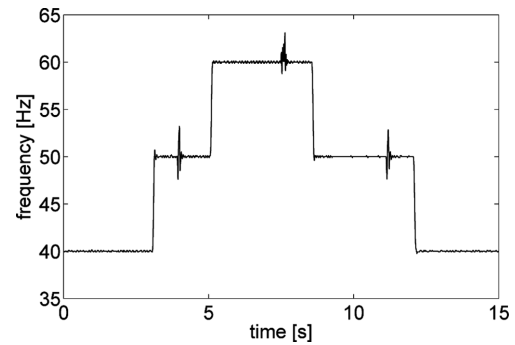Fig. 12 Frequency extracted with Sawyer-Tower circuit

Fig. 13 Averaged frequency extracted with Sawyer-Tower circuit

These diagrams are shown in Figs. 8-10 and 12. The frequency courses shown in Fig. 11 and Fig. 13 were obtained by averaging the frequency values over the last 50 ms at any time point. This method results in smoother curves with smaller errors. However, frequency changes are detected more slowly.

The experimental results show clearly that the frequency information of an external force component on an actuating piezoelectric transducer can be obtained by using self-sensing techniques. The best results are obtained from the bridge circuit with resistive reference branch. This may be due to better adjustability of this bridge circuit compared to the full capacitive bridge circuits. Although due to their linear characteristics bridge circuits are considered limited to the small-signal range for self-sensing the amplitudes of the mechanical quantities force and deflection their performance appears to be sufficient even in large-signal range if only frequency information is of importance. A successful transfer of the bridge circuit with a resistive reference branch onto the target system of the adaptronic strut for machine tools can be found in Munzinger (2007).

In addition to bridge circuits, a new approach of self-sensing the frequency information of an external force was verified. It directly exploits the circumstance of different frequency ranges by measuring and frequency filtering the charge on the transducer. Charge measurement was accomplished by a Sawyer-Tower circuit. This approach is insusceptible to detuning, its performance, however, turns out to be inferior to that of the bridge circuits. Furthermore, a frequency filter of higher order is necessary which introduces additional phase shift into the measuring chain. For use in control concepts for compensation of static and quasi-static signals this solution is appropriate, for extension of the frequency range of the

application, however, this phase shift must be regarded in the controller design. On the contrary, higher harmonics occurring due to nonlinearities of the piezoelectric material in large-signal operation have no significant influence on the operation behavior due to their small amplitudes. Since the overall results prove useful this concept can easily be transferred into the control system for the adaptronic strut shown in Fig. 2.

3. Design of control concept for adaptronic strut

Within this section different models of the adaptronic strut are presented. Starting with a simple three rigid body oscillator the control concept is developed and transferred to more complex models of the strut.

3.1. Three-body-oscillator

The strut within this model is simply considered to be consisting of three rigid bodies, the lower and the upper part of the strut and the piezoelectric transducer in-between. Using a lumped component approach, the system can be simplified as depicted in Fig. 14, where c_i, d_i and m_i define the material properties of the lumped bodies and F represents an external force.

With F_r being the force resulting from the piezoelectric actuator a, the equations of motion of the system read

$$\boldsymbol{M}\ddot{\boldsymbol{x}} + \boldsymbol{D}\dot{\boldsymbol{x}} + \boldsymbol{C}\boldsymbol{x} = \boldsymbol{f}F_r + \boldsymbol{f}_S F , \tag{11}$$

and rewritten in state space form

$$\dot{z} = \boldsymbol{A}z + \boldsymbol{b}u + b_S u_S \tag{12}$$

with state variable vector $z^T = [\dot{\boldsymbol{x}}^T, \boldsymbol{x}^T]$, $u = F_r$ and $u_s = F$.

3.1.1. Linear quadratic regulator

Using the analytical model in state space Eq. (12) a state controller for this single variable system is designed. The parameters are determined using the principle of a Least Quadratic Regulator (LQR).

The controller force then reads

$$F_r = -r^T z \tag{13}$$

while r is chosen to minimize the quadratic cost functional
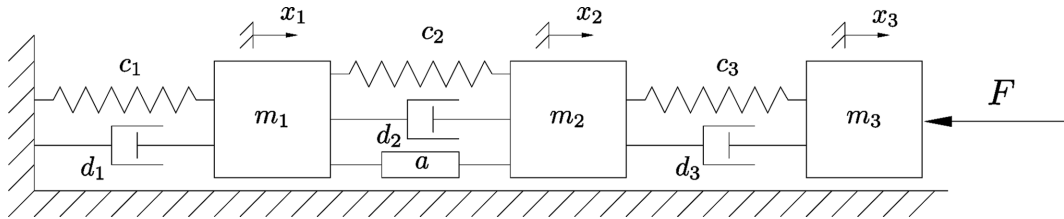

Fig. 14 Three-body oscillator

$$J = \frac{1}{2} \int_0^\infty \left[z^T(t) \boldsymbol{Q} z(t) + \frac{1}{k} F_r^2 \right] dt \ . \tag{14}$$

The solution of this minimization problem reads

$$\boldsymbol{r} = k\boldsymbol{b}^T \boldsymbol{P} \tag{15}$$

where $\boldsymbol{P}$ is the solution of the algebraic Riccati equation

$$\boldsymbol{PA} + \boldsymbol{A}^T\boldsymbol{P} + \boldsymbol{Q} - k\,\boldsymbol{P}\,\boldsymbol{bb}^T\boldsymbol{P} = 0. \tag{16}$$

The scalar $k > 0$ is a value for the cost of the controller input, $\boldsymbol{Q}$ is a positive, semi-definite matrix.
  The matrix $\boldsymbol{Q}$ is chosen as

$$\boldsymbol{Q} = \begin{bmatrix} w_{kin}\boldsymbol{M} & 0 \\ 0 & \boldsymbol{C} + \boldsymbol{C}^* \end{bmatrix} \tag{17}$$

such that $z^T\boldsymbol{Q}z$ represents a modified total energy of the system. The parameters w_{kin} and $\boldsymbol{C}^*$ represent weights for kinetic and potential energy, respectively. For more details on applying the LQR method and on setting the required parameters and weights, see Föllinger (1994), Lunze (2004), Preumont (2002) or Rudolf, *et al.* (2007).

3.1.2 Full state observer (Luenberger observer)

In general, the describing state vector of the system is not completely available. However, using a full state observer it can be estimated with a measured output y by

$$\hat{z} = \boldsymbol{A}\tilde{z} + \boldsymbol{b}u + l(\hat{y} - y), \tag{18}$$

where l is the observer feedback vector. The eigenvalues of a state controlled closed loop system ($\boldsymbol{A}$, $\boldsymbol{b}$, $\boldsymbol{r}$) are not shifted if an observer is inserted into the system. According to Föllinger (1994), their number is simply enhanced. Thus, as long as the plant is controllable and observable, the eigenvalues of controller and observer can be set separately. For realizing state control using a full state observer, the observer has to be faster in estimating the state vector than the controller. Using the pole assignment procedure according to Ackermann, Föllinger (1994), Tsui (2004), this can be achieved by placing the observer poles further on the left of the imaginary axis than the closed-loop controller poles, i.e.

$$\Re\{\lambda_{L^*}\} < \Re\{\lambda_{A^*}\}, \tag{19}$$

where λ_{L*} are the eigenvalues of the observer system $\boldsymbol{L}^* = \boldsymbol{A} - lc$ and λ_{A*} are the eigenvalues of the controller system $\boldsymbol{A}^* = \boldsymbol{A} - \boldsymbol{br}$.

3.1.3 Simulation results

For simulation the model of the three-body oscillator was built within the commercial multi-body soft-ware program Msc.Adams. The co-simulation interface between Adams and Matlab/Simulink was used for realizing controller and observer within the system. The exchange interval between the two
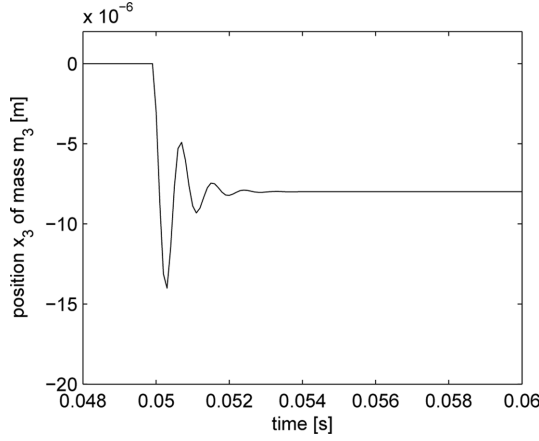
Fig. 15 LQR state controlled system under influence of external disturbance F=2 kN $\sigma(t$-0.05 s)

C – compensation element
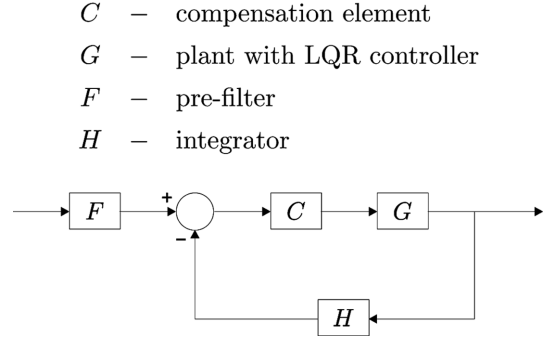G – plant with LQR controller
F – pre-filter
H – integrator

Fig. 16 Closed-loop system structure with integrator in feedback path

programs was set to $\Delta t = 0.1$ ms, which is identical to the maximum step size of the BDF integrator.

For the presented simulations the initial conditions of the system are zero velocities and positions, i.e. $z_i = 0$. The system is disturbed by the external force

$$F = 2 \text{ kN} \sigma(t - 0.05 \text{ s}).\tag{20}$$

For a chosen set of parameters w_{kin} and C^* according to Rudolf, *et al.* (2007) the simulation result of the controlled system is shown in Fig. 15. A steady-state control error is remaining.

To achieve a zero steady-state error an additional controller as shown in Fig. 16 shall be implemented. The plant including the LQR controller is represented by G, in the feedback path a simple integrator is placed, i.e. H=1/s. The pre-filter F which is only included for completeness is set to F=1. By adjusting the compensation element C using the root locus procedure, D'Azzo, *et al.* (2003), Lunze (2005), an optimal system behavior and a large stability margin can be achieved with dominating poles far away from the imaginary axis. It turns out that a simple proportional element for C is sufficient, Rudolf, *et al.*
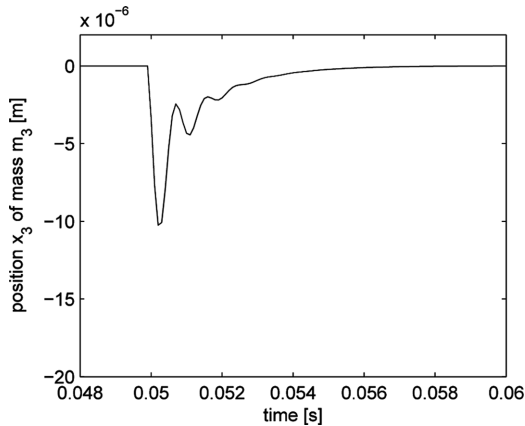

Fig. 17 LQR-PI state controlled system under influence of external disturbance force $F = 2$ kN $\sigma(t-$ 0.05 s)
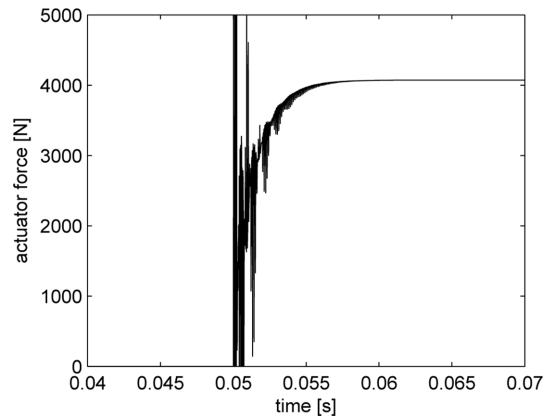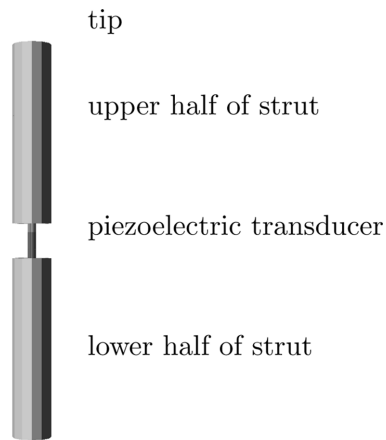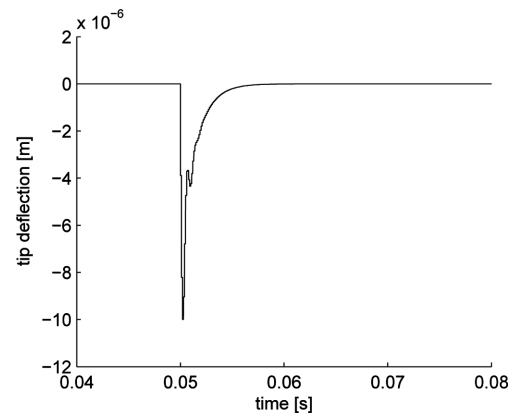

Fig. 18 Actuator force

Fig. 19 Simple model of adaptronic strut

Fig. 20 LQR-PI state controlled system under influence of external disturbance force $F = 2$ kN $\sigma(t$-0.05 s)

(2007).

In the following this combination of the LQR state controller, the integrator in the feedback path and the proportional element in the forward path is referred to as LQR-PI-controller. The efficiency of using both controller parts is shown in Fig. 17. There is no remaining steady-state error and the influence of the external force is compensated within less than 10 ms. The required actuator force for this control is depicted in Fig. 18.

3.2. Adaptronic strut by flexible bodies

Fig. 19 shows the first model including flexible bodies instead of lumped masses and lumped material properties. It comprises an upper and a lower half of the strut with the piezoelectric transducer in-between. The same control configuration with LQR and P-I elements is used for this model, whereas instead of the position x_3 of lumped mass m_3 the tip deflection of the upper half of the strut is used as control variable. The efficiency of the transfer of the control design under the influence of the same external disturbance force F is depicted in Fig. 20.

3.3. Adaptronic strut by CAD data

Using the design CAD data the exact geometry and exact material properties of the adaptronic strut can be considered in the flexible multi-body model shown in Fig. 21. Although this system is more complex the presented control configuration with LQR and P-I-elements is used with the tip deflection of the upper half of the strut being the control variable. This procedure was chosen since the design of a perfectly fitting control concept for this flexible multi-body model is rather laborious. The large number of modal coordinates required to describe the flexible behavior of the components result in a big number of state variables and thus, the handling gets costly and expensive. The response of the controlled system to the external disturbance force is depicted in Fig. 22.

The magnitude of the external force for this simulation was reduced by 1 kN, since the simple control model reaches its limits at F=1 kN for a step function when used for control of the complex model of the adaptronic strut. However, since mainly static and quasi-static loads are in focus of the application,

Fig. 21 Model of adaptronic strut by CAD data
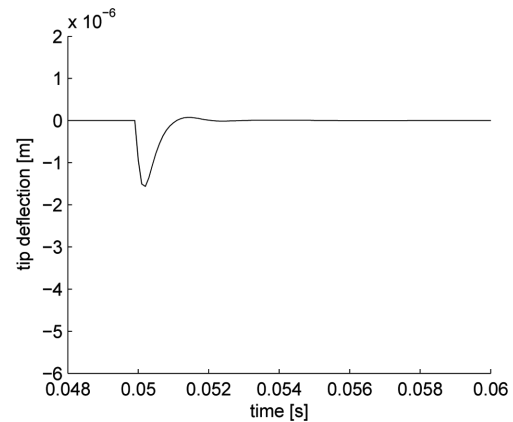
Fig. 22 LQR-PI state controlled system under influence of external disturbance force F=1 kN $\sigma(t-0.05$ s)

higher but slowly changing loads might still be compensated with the presented control concept. Further studies on this subject must be conducted. Additionally, investigations into the behavior of the adaptronic strut when built into the exemplary machine tool with parallel kinematics have to be done for evaluating the design and its transfer onto the complex model.

4. Adaptronic strut implemented in machine tool

Fig. 23 shows the exemplary machine tool with parallel kinematics where three conventional struts were exchanged by three adaptronic struts. Since both the compensation efficiency as well as the mechanical behavior of the machine tool depend on number and position within the machine tool of the substituted struts further investigations shall be conducted.

On one hand a substituted strut introduces an additional degree of freedom, allowing the correction of a small angular deflection of the TCP due to static or quasi-static loads. Thus, for turning processes one
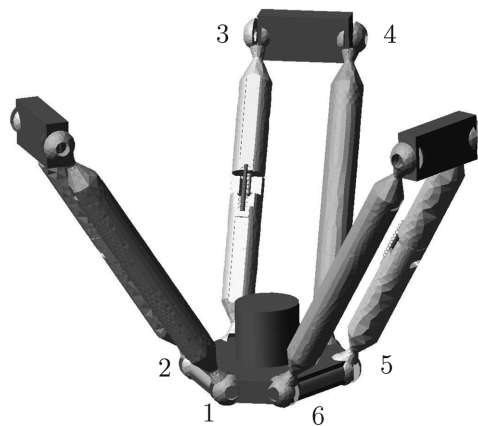

Fig. 23 Msc. Adams model of exemplary machine tool with parallel kinematics, exchanged adaptronic struts at positions 2,3,5 (ad235)
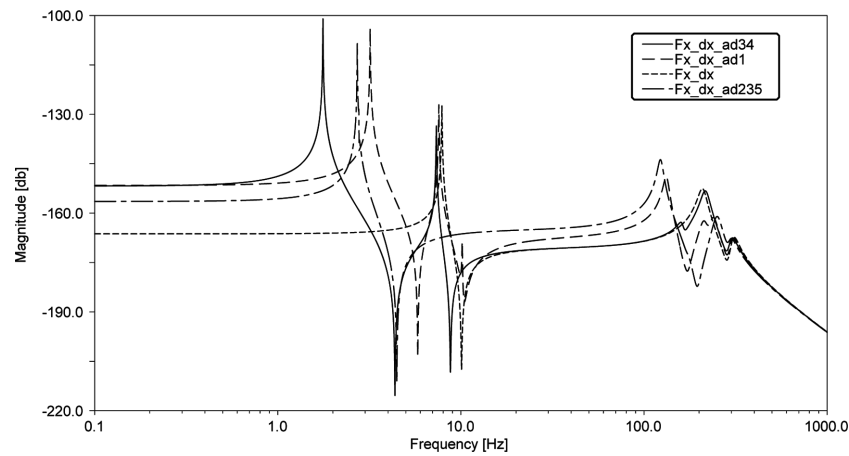
Fig. 24 Influence of number and position of adaptronic struts onto the stiffness of the machine tool, shown exemplarily by the frequency response G_{xx} of the position of the TCP to a process load
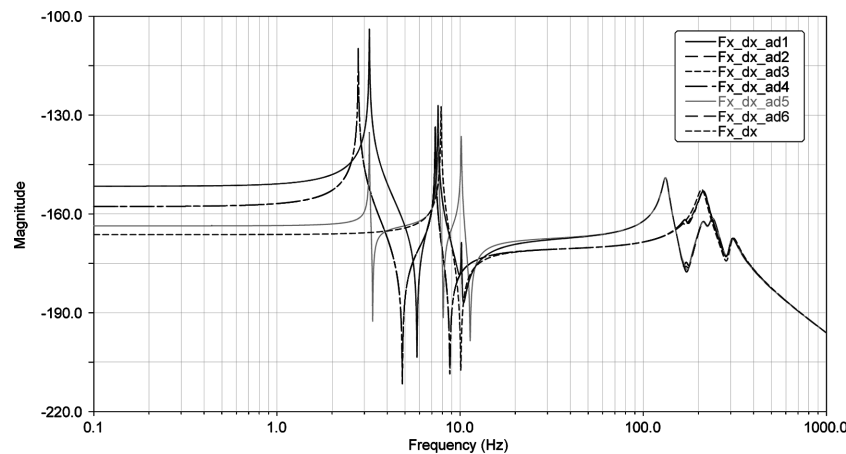

Fig. 25 Influence of position of adaptronic strut onto the stiffness of the machine tool, shown exemplarily by the frequency response G_{xx} of the position of the TCP to a process load

adaptronic strut might be sufficient since mainly point contact exists between tool and workpiece. For milling processes, however, usually planar contact between tool and workpiece occurs. Therefore, at least two adaptronic struts must be implemented into the machine tool. On the other hand, implementing the struts into the machine tool changes the stiffness of the machine tool. In a first step this influence is examined without controlling the strut. The frequency responses G_{xx} of the deflection of the TCP to a process load, that is acting on the TCP along the *x*-axis, depending on number and position of the adaptronic struts within the machine tool are depicted in Fig. 24 and Fig. 25.

As easily can be seen symmetries of the machine tool behavior due to it symmetric structure occur. The implementation of an adaptronic strut reduces the lowest resonance frequencies of the machine tool due to a decrease of its stiffness. The number of exchanged struts itself influences the stiffness only marginally as long as only one strut of each pair per guiding skid is exchanged.

The overall decrease of stiffness due to the implementation of the designed adaptronic strut is unwanted. By adding a second piezoelectric transducer and placing both elements off-center within the

Table 1 Constant deflections of TCP when strut number 4 is 10 μm longer than the other struts

dx [m]	dy [m]	dz [m]	φ_x [rad]	φ_y [rad]	φ_z [rad]
0	6.31e-6	8.73e-7	2.51e-9	-3.91e-5	3.06e-5

strut the stiffness of the adaptronic strut can be increased reaching the same magnitude as the original, conventional strut.

In the following the influence of a strut which is non-ideal and the influence of the position of the compensation unit on the considered machine tool are studied. Assuming strut number four according to Fig. 23 to be 10 μm longer than the other struts with the rest of the machine tool structure being ideal deflections of the TCP arise. These constant translational (d_x, d_y, d_z) and angular (φ_x, φ_y, φ_z) deflections with respect to the global coordinate system are listed in Table 1.

Depending on the position within the machine tool structure the in°uence of an adaptronic strut regarding the compensation of this geometric error varies. Therefore, the following examinations were accomplished. Starting from a parallel kinematic structure which originally was ideal apart from the elongation of strut number four strut i was regarded to be of adjustable length. While the machine tool has been at rest the length l_i of the strut was changed by elongations Δl_i with -30 μm $\leq \Delta l_i \leq$ 20 μm. The results are shown in Figs. 26-29. For reference, the olive colored graphs depict the constant deflections of the TCP due to the non-ideal strut 4 alone without any other influence.

As easily can be seen in the presented figures the influence of struts 2 and 6 on the deflections of the TCP are nearly equal. The same holds for the influence of struts 1 and 5. These similar effects are due to the rotational symmetry of the examined PKM machine tool. As shown in Fig. 26 and Fig. 27 all struts opposite to strut four (1,2,5,6) have similar influence on the translational deflections of the TCP. While the deflection d_y is set to zero by reducing the length of the corresponding strut the deflection d_z increases which is undesirable. However, this deflection can easily be compensated by moving all three guiding skids of the machine tool identically. Regarding the angular deflections of the TCP a similar behavior of these four struts (1,2,5,6) is found, as shown in Fig. 28 and Fig. 29. Here the reciprocal
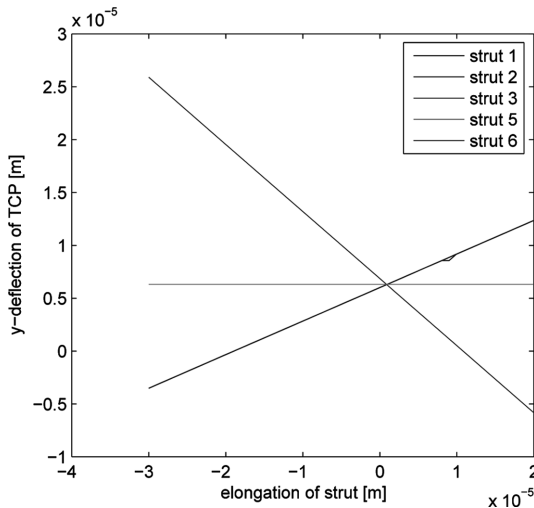

Fig. 26 *y*-deflection of the TCP due to Δl_4=10 μm and -30 μm $\leq \Delta l_i \leq$ 20 μm
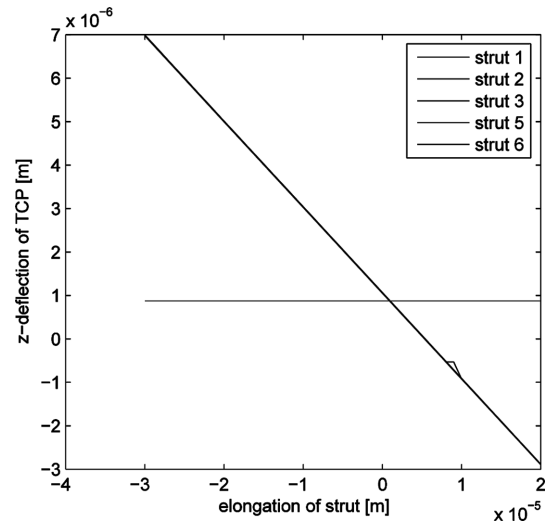
Fig. 27 *z*-deflection of the TCP due to Δl_4=10 μm and -30 μm $\leq \Delta l_i \leq$ 20 μm
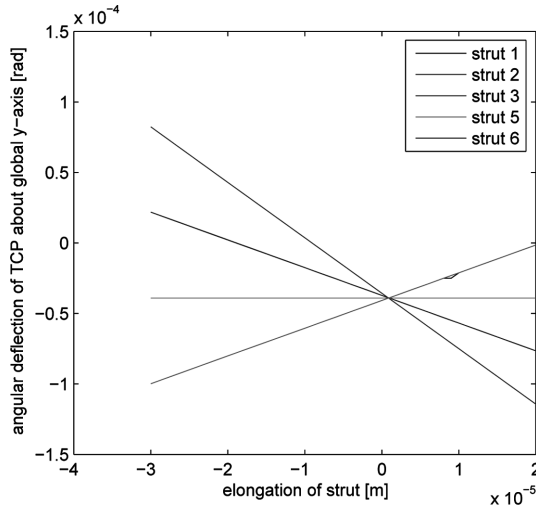
Fig. 28 Angular deflection φ_y of the TCP due to $\Delta l_4 =$
10 μm and -30 μm $\leq \Delta l_i \leq$ 20 μm
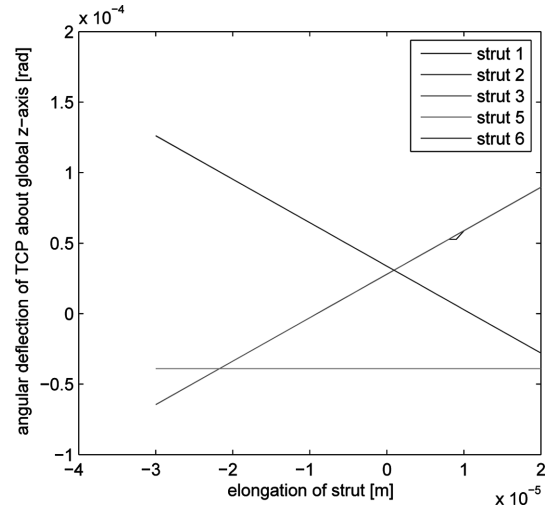
Fig. 29 Angular deflection φ_z of the TCP due to $\Delta l_4 =$
10 μm and -30 μm $\leq \Delta l_i \leq$ 20 μm

behavior can not be compensated by an additional movement of the guiding skid. Hence, the angular deflection of the TCP can only partially be reduced. This, however, might be sufficient, depending on the machining process. In turning processes there is only point contact between tool and workpiece, and thus, a single angular deflection might not affect the process and, therefore, the quality of the workpiece. Yet, if milling processes are considered such a deflection must be taken into account and one compensation unit might not be sufficient.

In this special case of a non-ideal strut 4 the best way for compensation is by making strut 3 adjustable in length. As long as both struts are of equal length all arising angular deflections can be compensated at all times by a position adjustment of the guiding skid corresponding to these two struts.

5. Conclusions

In this contribution an adaptronic strut for compensating static and quasi-static errors within machine tools with parallel kinematics has been presented. Using the functional principle of a scale with vibrating string static and quasi-static loads can be measured with piezoelectric transducers. For a better utilization of the limited size for the actuator element within the strut the usage of piezoelectric transducers as self-sensing actuators has been examined. Several different electrical circuits for acquiring the sensing signal while actuating simultaneously, such as capacitive and resistive bridge circuits and a Sawyer-Tower circuit, have been studied, verified, and evaluated by means of experimental results. Furthermore, a control concept has been developed and tested within three different models of the adaptronic strut: First a lumped parameter approach, second a flexible body approach and finally a model by CAD data. The evaluation of the presented control concept was accomplished by means of simulation results under external disturbance loads. At last, the static influence of number and position of the presented compensation unit within the machine tool was examined.

Intended future studies follow two parallel paths. Firstly, the presented electrical circuits shall be

integrated into the experimental test-rig of the adaptronic strut. Further studies of using the self-sensing properties of the piezoelectric transducer under loads comparable to loads during the machining process shall be conducted. Secondly, the controlled struts shall be implemented into the machine tool.

If more than one strut is substituted the extension of the presented single variable control to a multi variable control might be essential. Depending on the position of the TCP in the workspace of the machine tool the compensation of static and quasi-static errors shall be achieved. The efficiency of the strut shall be studied under machining processes such as turning and milling. Finally, an extension of the frequency range for compensating dynamic loads as well is envisaged.

Acknowledgements

References

Babuška, V. and O'Donnell, R. (1998), "Self-sensing actuators for precision structures", In *Aerospace Conf., 1998. Proc., IEEE.*

Bill, B. (2002), *Messen mit Kristallen: Grundlagen und Anwendungen der piezoelektrischen Messtechnik*, Verlag Moderne Industrie.

D'Azzo, J., Houpis, C. and Sheldon, S. (2003), *Linear Control System Analysis and Design with Matlab*, Taylor & Francis.

Fleischer, J., Knödel, A., Munzinger, C. and Weis, M. (2006), "Designing adaptronical components for compensation of static and quasi-static loads", In *Proc. of IDETC/CIE Conf., ASME, (DETC2006-99461).*

Föllinger, O. (1994), *Regelungstechnik*, Hüthig.

Janocha, H. and Kuhnen, K. (2002), "Real-time compensation of hysteresis and creep in piezoelectric actuators", *Sensor Actuat. A-Phys.*, **79**, 83-89.

Janocha, H. and Kuhnen, K. (2006), *Self-sensing effects in solid-state actuators*, In Encyclopedia of Sensors, American Scientific Publishers, **9**, 53-73.

Jones, L., Garcia, E. and Waites, H. (1994), "Self-sensing control as applied to a PZT stack actuator used as a micropositioner", *Smart Mater. Struct.*, **3**(2), 147-156.

Kuhnen, K. and Janocha, H. (2001), "Inverse feedforward controller for complex hysteretic nonlinearities in smart material systems", *Control Intel. Syst.*, **29**(3), 74-83.

Lunze, J. (2005), *Regelungstechnik 1*, Springer.

Lunze, J. (2004), *Regelungstechnik 2*, Springer.

Munzinger, C. (2007), *Adaptronische Strebe zur Steifigkeitssteigerung von Werkzeugmaschinen*, Shaker (in German).

Preumont, A. (2002), *Vibration Control of Active Structures - An Introduction*, Kluwer Academic Publishers.

Rudolf, C., Wauer, J., Fleischer, J. and Munzinger, C. (2005), "An approach for compensation of geometric faults in machine tools", In *Proc. IDETC/CIE Conf., ASME, (DETC2005-84241).*

Rudolf, C., Wauer, J., Fleischer, J. and Munzinger, C. (2006), "Measuring static and slowly changing loads using piezoelectric sensors", In *Proc. 10th Int. Conf. on New Actuators (P015).*

Rudolf, C., Wauer, J., Munzinger, C. and Weis, M. (2007), "Piezoelectric control of a machine tool with parallel kinematics", In *Proc. SPIE - Smart Structures and Materials and NDE Health Monitoring and Diagnostics, (6527-15).*

Ruschmeyer, K. (1995), *Piezokeramik*, expert verlag.

Tsui, C.C. (2004), *Robust Control System Design, Advanced State Space Techniques*, Marcel Dekker, Inc.

Xiang, H. and Shi, Z. (2009), "Static analysis of a multilayer piezoelectric actuator with bonding layers and electrodes", *Smart Struct. Syst.*, **5**(5), 547-564.